Molecular Cancer Therapeutics

β-Catenin Inhibitor BC2059 Is Efficacious as Monotherapy or in Combination with Proteasome Inhibitor Bortezomib in Multiple Myeloma

Ioanna Savvidou[1], Tiffany Khong[1], Andrew Cuddihy[2], Catriona McLean[3], Stephen Horrigan[4], and Andrew Spencer[1,5]

Abstract

Currently available treatment options are unlikely to be curative for the majority of multiple myeloma patients, emphasizing a continuing role for the introduction of investigational agents that can overcome drug resistance. The canonical Wnt/β-catenin signaling pathway, essential for self-renewal, growth, and survival, has been found to be dysregulated in multiple myeloma, particularly in advanced stages of disease. This provides the rationale for evaluating the novel β-catenin inhibitor BC2059 as monotherapy and in combination with proteasome inhibitors *in vitro* and *in vivo*. Here, we show nuclear localization of β-catenin in human myeloma cell lines (HMCL), consistent with activation of the canonical Wnt pathway. BC2059 attenuates β-catenin levels, in both the cytoplasm and the nucleus, reducing the transcriptional activity of the TCF4/LEF complex and the expression of its target gene axin 2. Treatment of HMCL with BC2059 inhibits proliferation and induces apoptosis in a dose-dependent manner. This is also observed in HMCL–stromal cell cocultures, mitigating the protective effect afforded by the stroma. Similarly, BC2059 induces apoptosis in primary multiple myeloma samples *in vitro*, causing minimal apoptosis on healthy peripheral blood mononuclear cells. Furthermore, it synergizes with the proteasome inhibitor bortezomib both in HMCL and primary multiple myeloma samples. Finally, in xenograft models of human myelomatosis, BC2059 delays tumor growth and prolongs survival with minor on-target side effects. Collectively, these results demonstrate the efficacy of targeting the Wnt/β-catenin pathway with BC2059 both *in vitro* and *in vivo*, at clinically achievable doses. These findings support further clinical evaluation of BC2059 for the treatment of multiple myeloma. *Mol Cancer Ther; 16(9); 1765–78.* ©*2017 AACR.*

Introduction

Multiple myeloma is an incurable neoplastic plasma cell disorder, accounting for approximately 1% of neoplastic diseases and 13% of hematologic cancers (1). Despite the improvement in progression-free and overall survival of multiple myeloma patients after the introduction of high-dose chemotherapy and stem cell rescue (autologous stem cell transplant) and more effective pharmacotherapies, the available treatment regimens are not curative (2). Thus, it is important to continue to identify and validate new therapeutic agents that target alternative pathways, which contribute to the pathogenesis and progression of multiple myeloma.

The canonical Wnt signaling pathway modulates the balance between stemness and differentiation in several adult stem cell niches, including hemopoiesis within the bone marrow (3). Furthermore, it is commonly dysregulated in a range of solid tumors including colon, liver, and pancreas carcinoma (4) and hematologic malignancies, including acute myeloid leukemia (4, 5), chronic myeloid leukemia (6), chronic lymphocytic leukemia (7), and multiple myeloma (8). In the absence of Wnt ligands, cytoplasmic β-catenin, which is the key player of the Wnt pathway, is constantly degraded by the Axin complex [comprised of axin, tumor suppressor adenomatous polyposis coli (APC), casein kinase 1 (CK1), and glycogen synthetase kinase 3 (GSK3)]. The amino terminal of β-catenin, upon phosphorylation by CK1 and GSK3, is subsequently recognized by an E3 ubiquitin ligase subunit, ubiquitinated and degraded by the proteasome. Thus, β-catenin is inhibited from reaching the nucleus where the Wnt target genes remain repressed under the influence of the DNA-bound T-cell factor/lymphoid enhancer factor (TCF/LEF) family of proteins. Conversely, upon binding of Wnt ligand to the seven-pass transmembrane Frizzled receptor (Fzd) and its coreceptor, low-density lipoprotein receptor related protein 6 (LRP6) or its close relative LRP5, Dishevelled protein (Dvl) phosphorylates LRP6, leading to the recruitment of the Axin complex to the cell membrane. As such, β-catenin remains unphosphorylated, accumulates in the cytoplasm, and then translocates into the nucleus, where it binds to the TCL/LEF complex initiating transcription of Wnt target genes (9).

Human myeloma cell lines (HMCL) and primary multiple myeloma cells have been shown to frequently express active,

[1]Myeloma Research Group, Australian Centre for Blood Diseases, Monash University/Alfred Hospital, Melbourne, Victoria, Australia. [2]Division of Cancer Research Peter MacCallum Cancer Center, Melbourne, Victoria, Australia. [3]Department of Anatomical Pathology, Alfred Hospital, Melbourne, Victoria, Australia. [4]BetaCat Pharmaceuticals, The University of Texas Health Science Center, Houston, Texas. [5]Malignant Haematology & Stem Cell Transplantation Service, Alfred Hospital, Melbourne, Victoria, Australia.

Note: Supplementary data for this article are available at Molecular Cancer Therapeutics Online (http://mct.aacrjournals.org/).

Corresponding Author: Andrew Spencer, Monash University/Alfred Hospital, Ground Floor, South Block, Commercial Road, Melbourne, Victoria 3004, Australia. Phone: 613-9076-3393; Fax: 613-9276-2298; E-mail: aspencer@netspace.net.au

doi: 10.1158/1535-7163.MCT-16-0624

nonphosphorylated nuclear β-catenin, whereas in normal B-cell subpopulations (naïve, germinal center, and memory B cells) and plasma cells, the nonphosphorylated form of β-catenin is undetectable (8, 10). In addition, IHC study of multiple myeloma bone marrow biopsies for nuclear expression of β-catenin has revealed strong β-catenin staining in the malignant plasma cells of 34% of multiple myeloma patients, where its presence was significantly correlated with more advanced disease stage (11). Furthermore, Wnt pathway genes (both upstream and downstream of β-catenin) have been found to be upregulated in multiple myeloma primary tumors when compared with normal plasma cells (10). However, in contrast to other malignancies, such as colon carcinoma or hepatocellular carcinoma, where the upregulation of the Wnt canonical pathway is due to mutations involving key components of the pathway, for example, APC, in multiple myeloma, no such mutations have been found; moreover, further activation of the pathway can be promoted by exposure to activators such as LiCl or Wnt3a, implying the existence of an intact, functional signaling pathway (10, 12). Consistent with this, evidence suggests that the aberrant activation of the Wnt canonical pathway may be secondary to the expression of Wnt ligands by both multiple myeloma and bone marrow stromal cells (BMSC; refs. 8, 10) frequently in parallel with coexpression of various Fz receptors and coreceptor LRP6 (12), and/or the hypermethylation of soluble Wnt inhibitor promoters (11, 13). Furthermore, recent data indicate that β-catenin can be further stabilized in multiple myeloma, especially in the nuclear compartment, by the process of SUMOylation (small ubiquitin-like modifier; ref. 14). SUMOylation is known to be aberrantly activated in multiple myeloma (15), and genetic inhibition of the process is able to increase the destruction of β-catenin by the ubiquitin–proteasome system (14). Overall, the available data confirming the upregulation of the Wnt canonical pathway in multiple myeloma, and its potential role in the proliferation, survival, and drug resistance of multiple myeloma cells, make it an attractive therapeutic target.

BC2059 (an anthracene-9,10-dione dioxime compound: 2-((3R,5S)-3,5dimethylpiperdin-1ylsulfonyl)-7-((3S,5R)-3,5-dimethylpiperidin-1-ylsulfonyl) (Supplementary Fig. S1) is a novel Wnt/β-catenin pathway inhibitor that has been shown to disrupt the binding of β-catenin to Transducin β-like protein 1 (TBL1) and its related protein (TBLR1), facilitating its destruction (16). TBL1 and TBLR1 were initially identified as members of the corepressor silencing mediator for retinoid and thyroid hormone receptor (SMRT)-nuclear receptor coreceptor (N-CoR) complex (17). Upon ligand binding, TBL1–TBLR1 mediate the exchange of the nuclear receptor corepressors, SMRT-N-CoR, for coactivators. In addition, TBL1–TBLR1 play a specific role in the recruitment of β-catenin to the Wnt target gene promoter. In the absence of Wnt ligands, the promoter region of the Wnt target genes is hypoacetylated due to the presence of the repressor complex (TCF, TLE1-HDAC1), whereas upon activation, β-catenin enters the nucleus, binds to TBL1–TBLR1, which preferentially binds to the hypoacetylated histones, thus localizing β-catenin to the region of the Wnt target gene promoter. Subsequently, β-catenin interacts with TCF, dissociating TLE1-HDAC1, thus inducing hyperacetylation that leads to the recruitment of coactivators and the initiation of transcription (18). Interestingly, SUMOylation of TBL1–TBLR1 can further potentiate interaction and transcriptional activation of β-catenin–TBL1–TBLR1 complex (19) and TBL1, besides acting as a transcriptional coactivator of β-catenin also protects β-catenin from degradation (20). In this study, we show that BC2059 has significant antiproliferative and proapoptotic effects on HMCL and primary multiple myeloma cells and can mitigate the protective/pro-proliferative effect of stromal cells, Wnt3a or conditioned media (CM) derived from multiple myeloma patient bone marrow stroma. The drug was confirmed to decrease β-catenin protein levels and the expression of downstream target genes; furthermore, BC2059 was shown to synergize with low doses of proteasomal inhibitors in killing multiple myeloma cells and was effective in a murine xenograft model of human multiple myeloma, thus providing a rationale for the further evaluation of the drug in the treatment of multiple myeloma.

Materials and Methods

BC2059 (2-((3R,5S)-3,5dimethylpiperdin-1ylsulfonyl)-7-((3S,5R)-3,5-dimethylpiperidin-1-ylsulfonyl) (16) was provided by BetaCat Pharmaceuticals. Bortezomib was purchased by assaymatrix, Melbourne, Australia. Investigations were conducted in accordance with the Declaration of Helsinki and acknowledged national and international guidelines and were approved by the Alfred Hospital Review Board.

Cell lines and culture conditions

HMCL U266, NCI H929, and RPMI8226 were obtained from the ATCC. OPM2 and LP1 cell lines were from Deutshe Samm-Lung von Mikroorgaanismen und Zellculturen. These cells were authenticated by the supplier using cytogenetics, DNA typing, immunophenotyping, and cell line speciation. Commercially available cell lines are purchased every 2 to 3 years. ANBL6, OCI-My1, and XG-1 were kind gifts from Dr. Frits Van Rhee (Winthrop P. Rockefeller Cancer Institute, Little Rock, AR) in 2008, whereas KMS11, KMS12 BM, KMS12 PE, and KMS18 were kind gifts from Kawasaki Medical School (Kurashiki, Japan) in 2008. The authors have confirmed that the cell lines are plasma cells by CD138, CD38, and CD45 by flow cytometry. HMCLs were grown and treated at densities between 2.0 and 2.5 $\times$ 10^5 cells/mL in RPMI1640 media (Gibco, Invitrogen) supplemented with 10% heat-inactivated FBS (Lonza) and 2 mmol/L L-glutamine (Gibco, Invitrogen). IL6-dependent cell lines were cultured with 2 to 5 ng/mL IL6 as required. All cells were cultured in a humidified incubator at 37°C with 5% CO_2 and used until 20th passage. All HMCLs were passaged 24 hours before the experimental setup to ensure high viability. Cell lines are screened every 2 months for mycoplasma contamination by VenorGeM Mycoplasma Detection Kit. The HMCLs were authenticated on December 2016 by CellBank Australia by the use of short tandem repeat profiling, in line with the standard ANSI/ATCC ASN-0002-2011, and matched publicly available data.

Immunoblotting and cell fractionation

HMCLs were fractionated using the NE-PER Nuclear and Cytoplasmic Extraction Reagents Kit (Thermo Fisher Scientific) as per the manufacturer's instructions. Protein concentration was quantified using the DC Protein Assay (Bio-Rad). Subsequently, 20 μg of each protein lysate was separated by 6% SDS-PAGE and blotted onto PVDF (Immobilon-P, Millipore) using the Bio-Rad wet transfer system. Membranes were blocked with 5% BSA 0.1% Tween-20/PBS for 60 minutes and then incubated with rabbit polyclonal anti-β-catenin (Cell Signaling Technology), mouse monoclonal anti-α-tubulin (Sigma-Aldrich), or

mouse monoclonal anti-TATA binding protein antibody (Abcam) overnight at 4°C or for 2 hours at room temperature. The blots were washed three times for 15 minutes with 0.1% Tween-20/PBS and then incubated with secondary horseradish peroxidase–tagged antibody (swine anti-rabbit Ig HRP or rabbit anti-mouse Ig HRP (Dako) for 1 or 2 hours at room temperature before washing as above. Blots were visualized with SuperSignal West Pico ECL reagents (Pierce, Thermo Fisher Scientific).

For β-catenin protein level measurement, KMS18 cells were treated with BC2059 at two different doses (IC_{50}, $1.5 \times IC_{50}$), and then at 16 hours, the cells were lysed with RIPA lysis buffer as described previously (21) or fractionated as per the manufacturer's instructions, and 70 or 30 μg of protein lysate was separated by 10% SDS-PAGE and blotted onto PVDF or nitrocellulose membrane, respectively (Hybond ECL, Amersham Biosciences). NCI H929 and U266 cells were treated with escalating doses of BC2059 for 20 hours and lysed with RIPA lysis buffer. Seventy micrograms of protein lysate was separated by 4% to 20% gradient precast gel (Min-Protean TGX gels, Bio-Rad) and blotted into PVDF. For β-catenin levels in HS5 stromal cells, 70 μg of KMS18 and HS5 protein lysate was separated by 6% SDS-PAGE. Membranes were blocked with 5% BSA, 0.1% Tween-20/PBS, or Odyssey Blocking Buffer (LI-COR Biosciences) and incubated first with rabbit polyclonal anti-β-catenin, mouse monoclonal anti-α-tubulin, or mouse monoclonal anti-TATA binding protein antibody, and then with secondary as above or with goat anti-rabbit (IRDy 800CW, LI-COR Biosciences) or goat anti-mouse (IRDy 680RD, IRDy800CW LI-COR Biosciences) according to the manufacturer's instructions. Total lysates blots were visualized with SuperSignal West Pico ECL reagents (Pierce, Thermo Fisher Scientific), whereas fractionated lysates blots were visualized on an Odyssey Infrared Imaging system, and densitometry was performed using the Image Studio software (Odyssey). Results were normalized to loading controls (α-tubulin or β-actin for the whole-cell lysates and cytoplasmic fractions and TATA binding protein for the nuclear fractions). Experiments were performed in triplicate.

Proliferation and viability assays

Proliferation was measured using the CellTiter 96 AQueous one solution cell proliferation assay (Promega) on a panel of 12 HMCLs. Cells were cultured at 2.0×10^5 cells/mL in 100 μL fresh media in 96-well plates for 24 and 72 hours with escalating concentrations of BC2059 (50–10,000 nmol/L). Twenty microliters of MTS reagent was added for the final 4 hours of treatment, and the plates were read at 490 nm using a Fluostar Optima plate reader (BMG Labtech). Parallely, cell viability of the treated HMCL was determined by Trypan blue staining and hemocytometer counts, and the degree of cell death was assessed by FACS with propidium iodine (PI) staining. To study the proapoptotic effect of BC2059, HMCLs were treated with increasing doses of the drug for 24 hours, and the cells were stained with FITC-Annexin V antibody (Molecular Probes by Life Technologies) for 30 minutes in the dark at room temperature, washed, resuspended in Annexin buffer, and acquired by FACS. Analyzed data represent the fold increase of Annexin V–positive cells divided by the positive Annexin V cells of the untreated sample. For the detection of cleaved PARP (cPARP), U266 HMCLs were treated with BC2059 for 24 hours. Cells were collected and fixed in 2% paraformaldehyde for 20 minutes at 4°C. Cells were then stained with FITC-cPARP (BD Biosciences) antibody in permeabilization buffer (PBS/0.1% saponin) for 30 minutes in the dark at room temperature, washed, resuspended in PBS, and acquired by FACS. Analyzed data represent the fold increase of cPARP-positive cells divided by the positive cPARP cells of the untreated sample. For the synergy experiments, 6 HMCLs were treated with BC2059 in combination with bortezomib for 24 hours before being harvested, resuspended in FACS buffer (0.5% heat-inactivated FBS in PBS) supplemented with 62.5 ng/mL PI (Sigma-Aldrich), and analyzed immediately by FACS. The proportion of PI-positive cells was quantitated by subtracting the background death of untreated cells. Cell death induced by single-drug treatment was compared with the combination treatment and combination indices (CI) calculated using the CalcuSyn software package (Biosoft). All experiments were performed at least in triplicate.

Coculture assays

HMCLs in isolation or in the presence of the immortalized stromal cell line HS5 were seeded at 2×10^5 cells/mL in 24-well plates and incubated for 4 hours in a humidified incubator at 37°C with 5% CO_2; then, varying concentrations of BC2059 were added, and the cells were incubated for a further 20 hours. Cells were trypsinized (TrypLE Express Enzyme, phenol red, Gibco Life Technologies), washed with PBS, and stained with CD10 FITC (Beckman Coulter) for 30 minutes at 4°C. Unbound antibody was washed off, and the cells were resuspended in FACS buffer (0.5% heat-inactivated FBS in PBS) supplemented with 62.5 ng/mL PI (Sigma-Aldrich) and analyzed immediately by FACS. The proportion of PI-positive $CD10^+$ (HS5) and $CD10^-$ (HMCL) cells was quantitated by subtracting the background death of untreated cells. For BMSC CM preparation, bone marrow mononuclear cells (BMMC) from 3 multiple myeloma patients were isolated from heparinized aspirates by Ficoll gradient, pooled, resuspended in 10% FBS DMEM media, and incubated for 24 hours, after which the supernatant was removed and the adherent cells were then grown in 10% FBS until 80% confluence was achieved. The medium was then removed, and cells were incubated for another 48 hours in serum-free DMEM. The CM1 was then centrifuged and stored at −80°C for later use. The experiment was repeated with 3 additional multiple myeloma patients' derived BMSC CM (CM2). Subsequently, NCI H929 were starved overnight, resuspended in serum-free medium (SFM) or CM at 2×10^5 cells/mL, and incubated for 4 hours. BC2059 was then added and the cells were incubated for a further 16 hours. Viable cell numbers were then determined by Trypan blue staining and hemocytometer count. Similarly, for Wnt3a and Wnt5a stimulation, NCI H929 were starved overnight, resuspended at 2×10^5 cells/mL in SFM, and treated with 100 nmol/L of rhWnt3a or 100 or 200 nmol/L of rhWnt5a (both R&D Systems). After 4 hours, BC2059 was added and cells were incubated for a further 16 hours and viable cell numbers enumerated with Trypan blue staining and hemocytometer count. All experiments were performed in triplicate.

Primary samples

Primary multiple myeloma samples were obtained from relapsed and refractory multiple myeloma patients, following written informed consent with approval from the Alfred Hospital Research and Ethics Committee. BMMCs were isolated with Ficoll-Paque Plus (Amersham Biosciences) and washed in PBS, and red blood cells were lysed with NH_4Cl solution (8.29 g/L ammonium chloride, 0.037 g/L ethylene diamine tetra-acetic

acid, and 1 g/L potassium bicarbonate). Cells were then washed with PBS, quantitated by hemocytometer, and subsequently cultured in RPMI1640 media supplemented with 10% heat-inactivated FBS and 2 mmol/L L-glutamine for 24 hours. The percentage of multiple myeloma cells was quantified by CD45 and CD38 staining by FACS. The next day, cells were plated at 2.5 $\times$ 10^5 multiple myeloma cells/mL and treated with BC2059 (250–1,000 nmol/L) alone or in combination with bortezomib (10–40 nmol/L) for 24 and 72 hours. Drug-induced multiple myeloma–specific cell apoptosis was then compared with untreated controls by staining for CD45 FITC (BD Biosciences), CD38 PerCP-Cy5.5 (BD Biosciences), and Apo 2.7 PE (Immunotech Beckman Coulter) followed by FACS analysis.

Super TOP-/FOP-FLASH Wnt reporter

KMS11 cells (1×10^5) were transfected with Super 8xTOP-FLASH or Super 8xFOP-FLASH Wnt reporter plasmids (a gift from Randall Moon, Addgene, plasmid 12456 and 12457) containing wild-type or mutant TCF DNA-binding sites by using Lipofectamine 2000 (Invitrogen, Life Technologies) according to the manufacturer's instructions and cotransfected with the pRL-TK vector (Promega) as an internal control reporter vector. Cells were then treated with rhWnt3a for 8 hours before treatment with BC2059 for an additional 12 hours. Reporter activity was then assessed by using the Dual Luciferase Assay System (Promega). Results were normalized to *Renilla* values for each sample. The reporter assay results represent the average of two independent transfection experiments.

qRT-PCR

The primer sequences for the *AXIN2* and *BIRC5* (the gene encoding survivin) qRT-PCR were:

forward GCCGATTGCTGAGAGGAACTG
reverse AAAGTTTTGGTATCCTTCAGGTTCAT,
forward AGAACTGGCCCTTCTTGGAGG
reverse CTTTTTATGTTCCTCTATGGGGTC.

KMS18 cells were treated with BC2059 for 16 hours and NCI H929 and U266 for 20 hours. Total RNA from untreated and treated cells was prepared using Qiagen RNeasy Mini Kit (Qiagen), and any residual genomic DNA was removed utilizing the Turbo-DNase I Kit (Ambion). Reverse transcription was performed on 1,000 ng of total RNA with 100 U of Superscript III reverse transcriptase (Life Technologies) and random hexamers (Life Technologies, 2.5 μmol/L final concentration), according to the manufacturer's guidelines. The reaction mixture consisted of 8 μL of Power-SYBR PCR Master Mix (Life Technologies) with 500 nmol/L of each forward (F) and reverse (R) primers for target gene and 2 μL of diluted template cDNA. PCR was performed with a LightCycler 480 Real-Time PCR machine (Roche) at 95°C for 10 minutes, with 45 cycles of amplification 95°C for 15 seconds, 62°C for 30 seconds, and 72°C for 30 seconds. All experiments were performed in triplicate, and each test sample was run in duplicate. For sample loading normalization, β-actin (*ACTB*; encoding β-actin) was used. Amplified products were all verified by melting curves analysis. Data were analyzed using SDS software version 2.3 (Life Technologies), and copy number of target genes was determined by the comparative threshold cycle method ($\Delta\Delta C_t$) using the Pfaffl method. Data are presented as mean ± SEM.

β-Catenin knockdown

For β-catenin knockdown, 2 mL of 2×10^5/mL KMS18 cells were plated into a 12-well plate at day 0 (KMS18 doubling time: 36 hours). At day 1, media were replaced by 1 mL of Opti-MEM (Gibco Opti-MEM I Reduced Serum Medium, Thermo Fisher Scientific), and transfection was carried out with Lipofectamine RNAiMAX (Thermo Fisher Scientific) according to the protocol provided by the manufacturer. For β-catenin knockdown, we used SignalSilence β-catenin siRNA I and β-catenin siRNA II (Cell Signaling Technology) at concentrations recommended by the manufacturer, whereas Silencer Negative Control No. 1 siRNA (Thermo Fisher Scientific) was used as a negative control, at the same concentration. Six hours after the transfection, 1 mL of fresh media (RPMI-10% FCS) was added in every well. At days 2 and 3, cells were treated with BC2059 (50, 100, 150 nmol/L) and then harvested at day 4 (72 hours after transfection). Cell death was monitored by PI staining with FACS, whereas untreated cells were collected for β-catenin protein level measurement by immunoblotting. Cells were lysed with RIPA lysis buffer, and 70 μg of protein was separated by 6% SDS-PAGE and blotted onto PVDF as already described. β-Actin (mouse mAb HRP conjugate; Cell Signaling Technology) was used as a loading control.

In vivo studies

Approval for the murine studies was obtained from the Animal Ethics Committee of the Alfred Hospital, Melbourne, Australia (E/1376/2031/M). Adult age-matched Cg-Prkdcscid Il2rgtm1Wjl/SzJ mice (The Jackson Laboratory) were injected (intravenously) with 1×10^6 U266 HMCL, carrying the FUL2-TGvector (a generous gift from Dr. Marco Herold, WEHI, Melbourne, Australia; with luciferase2 and GFP under the constitutively active ubiquitin and IRES promoter, respectively). At day 21, a limited course of treatment was commenced after confirmation of established measurable disease by bioluminescence. Control mice ($n = 4$) received 17% Solutol HS 15 (Sigma-Aldrich), whereas treated mice received 5 ($n = 4$) or 10 mg/kg BC2059 ($n = 5$) twice a week intravenously for 3 consecutive weeks (6 doses in total). Tumor burden was monitored on a weekly basis by *in vivo* imaging, from the second week of the experiment (day 18) until the first mice reached scientific endpoints. Briefly, mice were anaesthetized, injected intraperitoneally with 125 mg/kg luciferin, and imaged with the Lumina III XR system (PerkinElmer). Acquisition and analysis were performed with the Living Image system. Peripheral blood counts were evaluated sequentially during the course of the experiment (Hemavet, Drew Scientific, Inc.). Upon reaching scientific endpoints (e.g., hind limp paralysis, >20% weight loss), mice were humanely euthanized and tissues (skin and colon) were collected. Tissues were formalin fixed and embedded in paraffin, sectioned, and stained with H&E and β-catenin antibody. Images were taken with an Olympus BX51 microscope.

Statistical analysis

Statistical analysis was performed using GraphPad Prism 6 (GraphPad Software, Inc.).

Results

Targeting the dysregulated Wnt/canonical pathway by BC2059 induces apoptosis in HMCL

We first evaluated β-catenin expression pattern in a panel of 12 genetically heterogeneous HMCLs and confirmed the presence

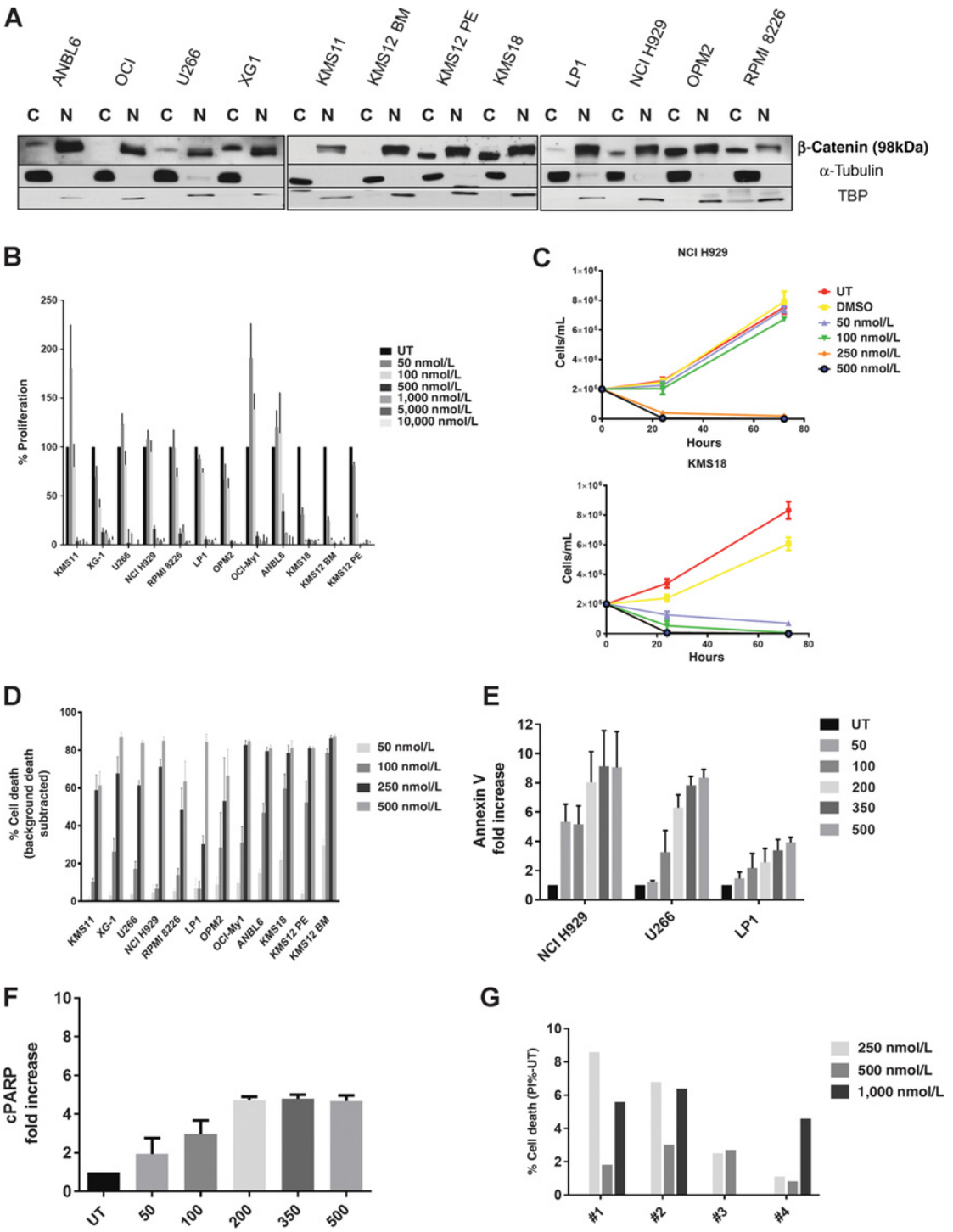

Figure 1.

Wnt canonical pathway is active in HMCLs, whereas its inhibition with BC2059 induces arrest of proliferation and apoptotic cell death, with minimal effect on healthy PBMCs. **A,** Nuclear (N) and cytoplasmic (C) fractions of HMCL. Loading control, α-tubulin-cytoplasmic, anti-TATA binding protein (TBP)-nuclear. **B,** BC2059 inhibits HMCL proliferation in a dose-dependent manner. Twelve HMCLs were cultured for 24 and 72 hours untreated (UT), or with BC2059 (50, 100, 500, 1,000 nmol/L). Cell proliferation was then determined by MTS assay (24-hour data shown, $n = 3$–6, mean ± SE). **C,** Absolute cell numbers of viable cells were determined by hemocytometer counts of HMCL cultured alone (UT), with BC2059 (50, 100, 250, 500 nmol/L) or with vehicle. BC2059 greatly decreased the proliferation of the 12 HMCLs over 72 hours (NCI H929 and KMS18 data shown, $n = 3$, ± SE). **D,** BC2059 induces cell death in HMCL. Proportion of PI^+ cells after BC2059 treatment for 24 hours. Data shown are the mean of three to four independent experiments ± SE. **E,** BC2059 induces apoptosis in HMCL. Annexin V–positive cells after BC2059 treatment for 24 hours, in three HMCLs ($n = 3$, ± SE). **F,** BC2059 induces cleavage of PARP. cPARP-positive cells were determined by FACS, after treatment of U266 HMCL with BC2059 for 24 hours ($n = 3$, ± SE). **G,** BC2059 has minimal toxicity on healthy PBMCs.

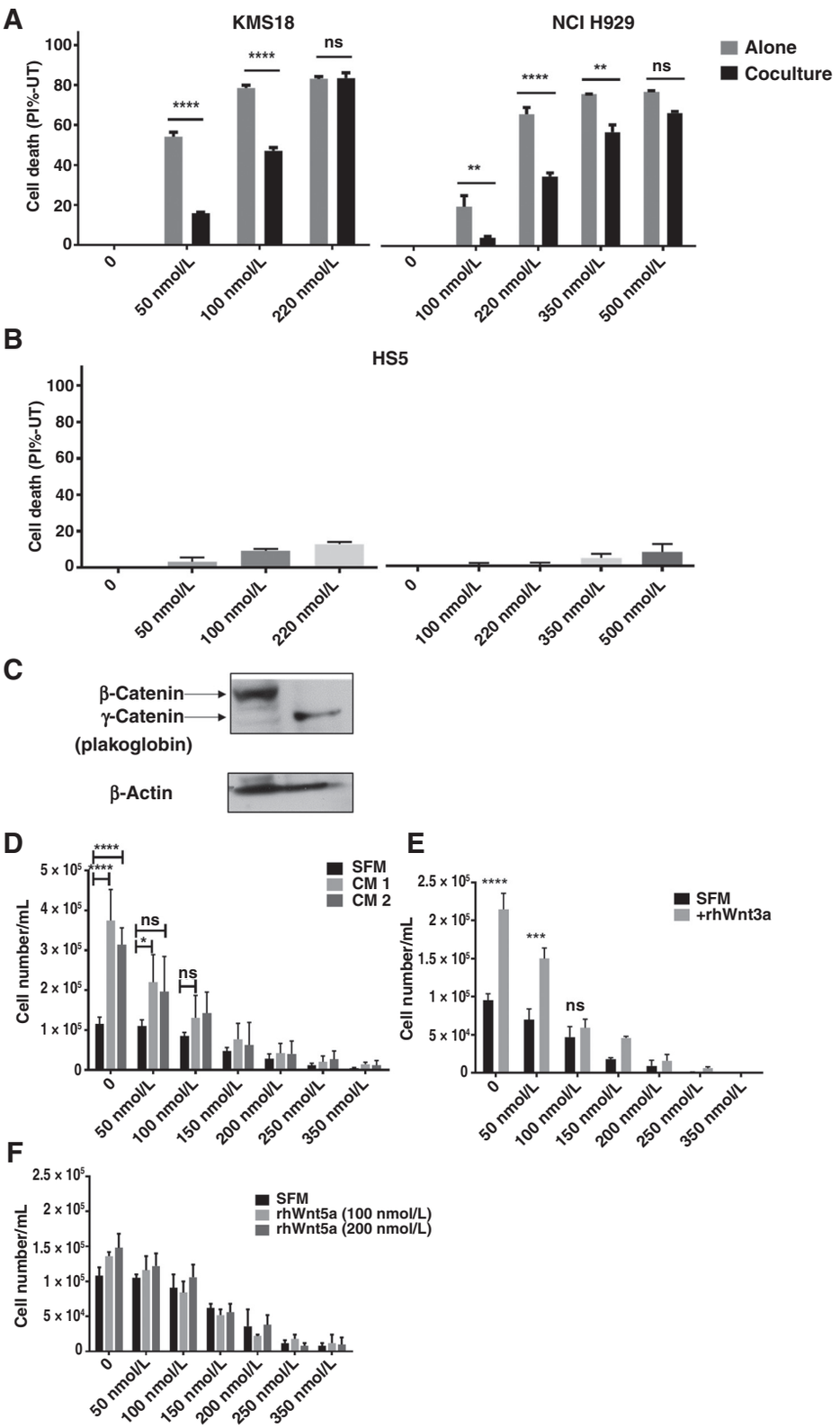

Figure 2.

Treatment of HMCL with BC2059 mitigates the antiapoptotic and pro-proliferative effect of the stroma and Wnt canonical pathway stimulation. **A,** Two HMCLs (KMS18, NCI H929) were cultured either alone or with stromal cells (HS5) and treated with BC2059 for 24 hours, up to IC_{80} and cell death of HMCL calculated ($n = 3$, ± SE, results analyzed using a two-way ANOVA with Bonferroni posttest; **** = $P < 0.0001$; ** = $P < 0.01$, ns = $P > 0.05$). **B,** HS5 stromal cell death was calculated in the coculture experiment ($n = 3$, ± SE). **C,** β-Catenin expression in HS5 stromal cells compared with that in an HMCL (KMS18). Loading control, β-actin. The blot shown is the representative of two biological replicates. **D,** NCI H929 were cultured in SFM, CM1, or CM2 4 hours before the addition of BC2059 (50, 100, 150, 200, 250, 350 nmol/L), and 16 hours later, viable cell numbers were determined by hemocytometer counts ($n = 3$, ± SE, results were analyzed using a two-way ANOVA with Bonferroni posttest; **** = $P < 0.0001$; * = $P < 0.05$, ns = $P > 0.05$). **E,** Similarly, the pro-proliferative effect of the addition of rhWnt3a (100 nmol/L) on NCI H929, in terms of viable cell numbers was overcome by the addition of BC2059 (50, 100, 150, 200, 250, 350 nmol/L) for 16 hours ($n = 3$, ± SE, results were analyzed using a two-way ANOVA with Bonferroni posttest; **** = $P < 0.0001$; *** = $P < 0.001$; ns = $P > 0.05$). **F,** In contrast, the addition of rhWnt5a (100 and 200 nmol/L) on NCI H929 did not demonstrate a pro-proliferative effect ($n = 3$, ± SE, results were analyzed using a two-way ANOVA with Bonferroni posttest).

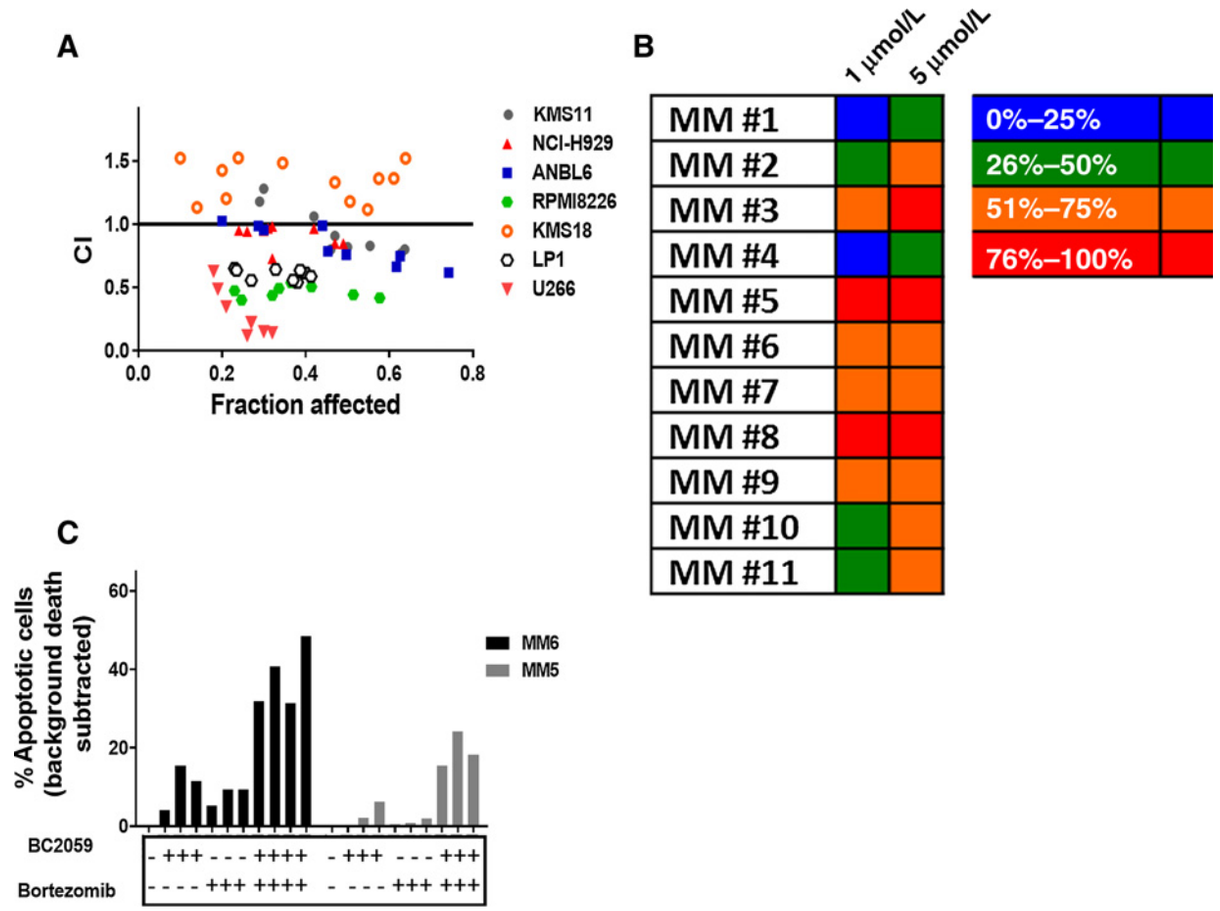

Figure 3.

BC2059 synergizes with bortezomib against HMCL and induces apoptosis of primary multiple myeloma (MM) samples as a single agent and in combination with bortezomib. **A,** BC2059 (IC_{20}–IC_{40}) in combination with bortezomib (4–12 nmol/L) demonstrated synergism against HMCL ($n = 3$). Synergy was measured using the CI calculated by CalcuSyn software, in which values less than 1 represent synergism. CI was plotted against the fraction of the HMCLs killed with the various used doses after 24 hours. **B,** Proportion of apoptotic (Apo 2.7 +) $CD38^+$ $CD45^-$ primary multiple myeloma cells in an autologous bone marrow coculture assay after 72 hours of BC2059 treatment with 1 and 5 μmol/L ($n = 11$). **C,** Proportion of apoptotic (Apo 2.7 +) $CD38^+$ $CD45^-$ primary MM cells after 24-hour BC2059 and/or bortezomib treatment ($n = 2$).

of nuclear β-catenin in all cases (Fig. 1A), signifying the dysregulation of the canonical pathway in multiple myeloma. The presence of two closely situated bands on immunoblotting implied the presence of both an unphosphorylated (lower migrating band) and phosphorylated β-catenin (higher migrating band) moieties. The antiproliferative impact of BC2059 was confirmed by MTS assay (Fig. 1B), demonstrating that by 24 hours, all 12 HMCLs treated with 500 nmol/L BC2059 had less than 15% metabolic activity. The extent of the inhibitory effect of BC2059 was then recapitulated by quantitation of viable cell number with Trypan blue staining in two HMCLs (NCI H929 and KMS18), showing marked reductions in viable HMCL numbers at both 24 and 72 hours following treatment (Fig. 1C). We then demonstrated the cytotoxic effect of BC2059 in all 12 HMCLs. Cell death was evident at both 24 (Fig. 1D) and 72 hours (Supplementary Fig. S2) following treatment with BC2059 with an LD_{50} of <250 nmol/L demonstrated for 11 of 12 HMCLs. The proapoptotic effect of the drug was validated by the measurement of Annexin V staining on three HMCLs with different sensitivities to the drug (NCI H929 and U266: intermediate sensitivity, LP1: resistant). Escalating doses of BC2059 were able to increase the proportion of Annexin V–expressing cells in every cell line tested (Fig. 1E). Furthermore, in U266, BC2059 was able to upregulate the expression of cPARP (Fig. 1F), a known marker of apoptosis, downstream of active caspase-3, confirming the proapoptotic effect of the drug. BC2059 had minimal toxicity when tested against normal PBMCs, with median cell death at 1,000 nmol/L at 24 hours of only 5% (Fig. 1G).

BC2059 mitigates the protective antiapoptotic and proproliferative effect of both BMSCs and exogenous Wnt3a

Multiple myeloma benefits from bone marrow microenvironmental signals that promote survival, proliferation, and drug resistance. Of specific relevance to the current study, BMSCs have been found to secrete Wnt ligands that likely contribute to the observed dysregulation of the Wnt/β-catenin pathway in multiple myeloma (5). We therefore evaluated the pronecrotic effect of BC2059 on NCI H929 and KMS18 cultured with HS5. Baseline cell death of HMCLs was similar in both conditions (alone or

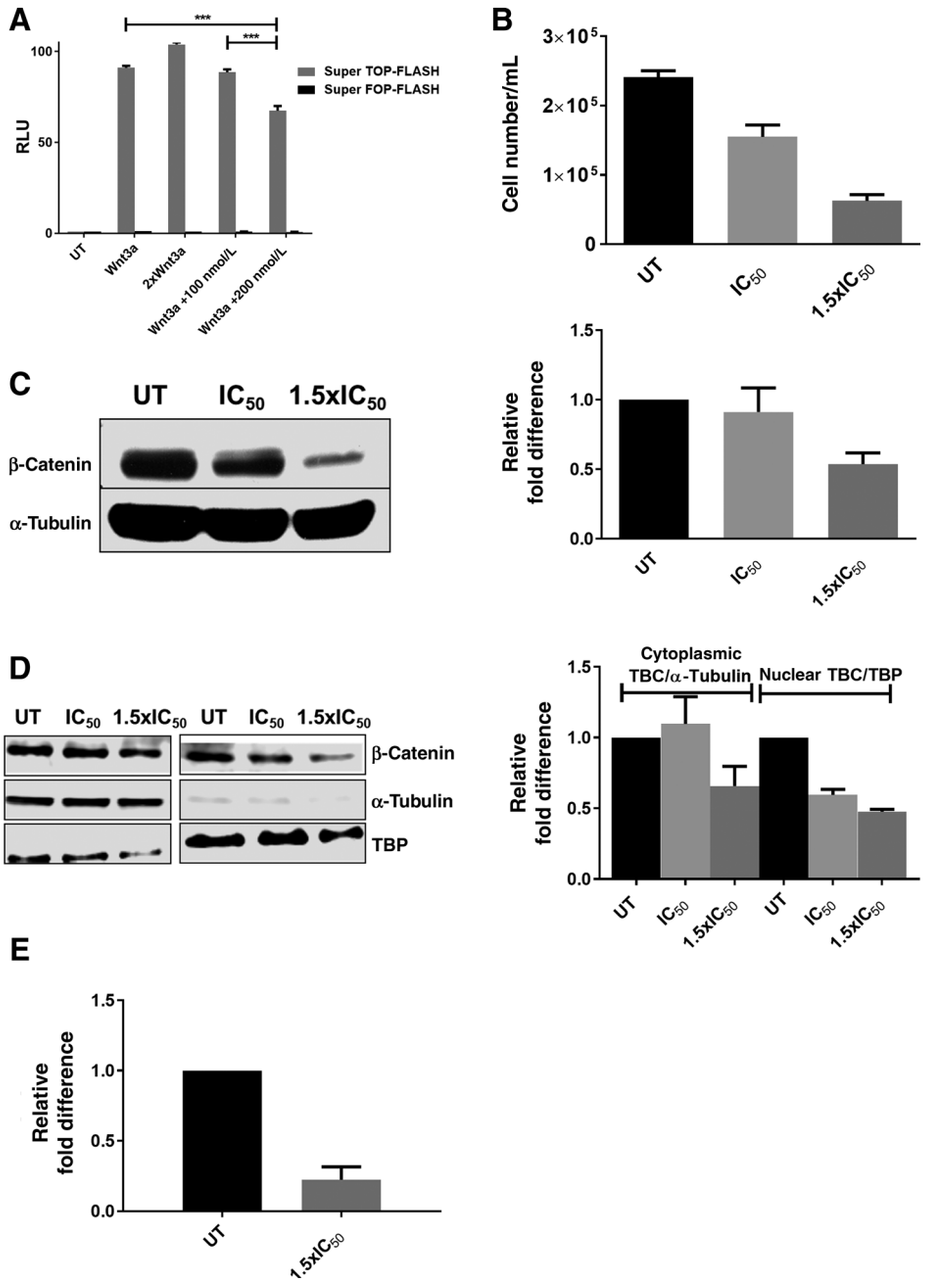

Figure 4.
BC2059 inhibits the activity of the β-catenin/TCF transcriptional complex and facilitates β-catenin destruction. **A,** KMS11 endogenous reporter activity is enhanced on addition of rhWnt3a but blocked by BC2059. RLU = relative light units ($n = 2$, mean ± SE, transfected cells stimulated with rhWnt3a and treated with BC2059 were analyzed using one-way ANOVA with Tukey posttest). **B,** BC2059 causes apoptosis of KMS18 cells at 16 hours at doses equal to IC_{50} and 1.5 × IC_{50}. 2 × 10^5 KMS18 cells were left untreated or treated with BC2059 (IC_{50}, 1.5 × IC_{50}, IC_{50}: 73 nmol/L), and 16 hours later, absolute cell numbers of viable cells were determined by hemocytometer counts ($n = 4$). **C,** Immunoblotting of whole-cell lysates from untreated and treated KMS18 cells and densitometric analysis showed a significant reduction of total β-catenin protein expression at 1.5 × IC_{50} ($n = 4$). Loading control: α-tubulin. **D,** BC2059 treatment of KMS18 cells for 16 hours promotes the destruction of the nuclear (active) β-catenin [total β-catenin (TBC)] and to a lesser extent that of the cytoplasmic (inactive) β-catenin [total β-catenin (TBC)]. Immunoblot of cytoplasmic and nuclear fractions of KMS18-treated cells and densitometric analysis of β-catenin levels ($n = 3$). Loading controls: α-tubulin, cytoplasmic, TATA-binding protein (TBP), nuclear. **E,** Decreased β-catenin protein expression correlates with downregulation of the downstream target gene axin 2. KMS18 cells ($n = 3$) were treated for 16 hours with 1.5 × IC_{50}.

coculture) for both cell lines tested (NCI H929 alone: 13% ± 2.68%, coculture: 16% ± 1.34%, KMS18 alone: 11.13% ± 0.4%, coculture: 11.7% ± 1.1%). At low doses of the drug, stromal cells significantly protected HMCL from cytotoxicity, whereas the addition of BC2059 at doses equal to IC_{80} mitigated the prosurvival effect of the stromal cells, with >50% cell death achieved in both cases (Fig. 2A). Cell death of the stromal cells by the drug did not exceed 14.8% at the highest doses (500 nmol/L) both when cultured alone and in the coculture system (Fig. 2B). BC2059's lack of cytotoxicity on HS5 stromal cells could be attributed to the undetectable levels of β-catenin protein in these cells (Fig. 2C), when compared with an HMCL (KMS18). Similarly, the growth advantage of NCI H929 when cultured with CM derived from multiple myeloma-patients (CM1 and CM2; Fig. 2D) or rhWnt3a (Fig. 2E) was inhibited by BC2059 in a dose-dependent fashion. Interestingly, exposure to rhWnt5a ligand, a known activator of the noncanonical pathway, under the same conditions had no proliferative effect on NCI H929 (Fig. 2F).

BC2059 induces apoptosis of primary multiple myeloma cells and synergizes with bortezomib

To assess the potential of BC2059 for future combination treatment approaches, HMCLs were treated with BC2059 and the proteasome inhibitor bortezomib at a range of doses and the presence of synergy calculated using CalcuSyn software (CI < 1 defines synergism). For 6 of 7 HMCLs, the combination was

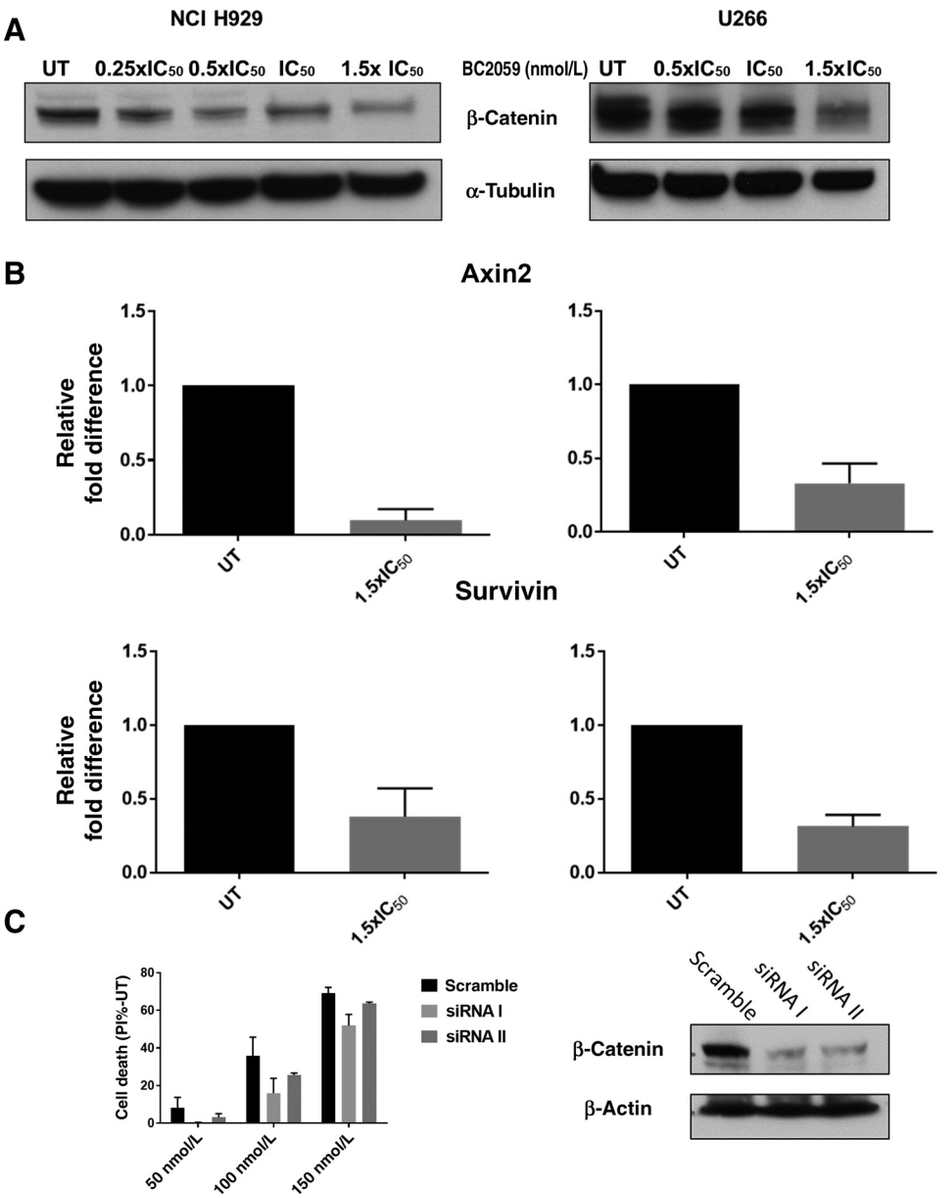

Figure 5.
BC2059 inhibits the transcription of downstream target genes of β-catenin and shows specificity for β-catenin. **A,** BC2059 treatment of NCI H929 (IC_{50}: 173 nmol/L) and U266 (IC_{50}: 186 nmol/L) cells for 20 hours promotes the decrease of total β-catenin protein. **B,** NCI H929 and U266 cells treated with 1.5 × IC_{50} of BC2059 for 20 hours show decreased transcription of β-catenin target genes *AXIN2* (top) and *BIRC5* (survivin) mRNA (bottom). **C,** β-Catenin knockdown was performed in KMS18 HMCLs, and the cells were treated for 2 consecutive days with escalating doses of BC2059. Cell death was monitored by PI^+ staining, 72 hours after transfection ($n = 3$ ±SE; left). β-Catenin protein level was evaluated 72 hours after transfection by immunoblotting. β-Catenin siRNA I and siRNA II transfected cell lysates were compared with the negative control siRNA lysate (scramble). β-Actin: loading control.

synergistic or additive with doses ranging from IC_{20} to IC_{40} for BC2059 and 4 to 12 nmol/L for bortezomib. This included the HMCL most resistant to single-agent BC2059, LP1 (IC_{50}: 320 nmol/L). Only KMS18, which was exquisitely sensitive to single-agent BC2059 (IC_{50}: 73 nmol/L), could not demonstrate synergy (Fig. 3A). The effect of BC2059 on *ex vivo* primary multiple myeloma cells was similarly evaluated both as a single agent and in combination with bortezomib. Primary multiple myeloma tumor cells derived from 11 patients with relapsed and/or refractory multiple myeloma were treated for 72 hours, after which the $CD38^+CD45^-$ multiple myeloma cell population was assessed for apoptosis by flow cytometry (Fig. 3B). The median cell death at 1,000 nmol/L was 50.05%, ranging from 17% to 90%, with 42% of samples demonstrating an LD_{50} of <1,000 nmol/L to single-agent BC2059. The combination of BC2059 and bortezomib was tested against two primary multiple myeloma tumor samples (Fig. 3C). In both cases, BC2059 synergized with bortezomib, with synergy quotients (SQ) ranging from 1.3 to 8.2 (where SQ >1 defines synergism). Interestingly, one of the tumors that was refractory to bortezomib both *in vivo* (patient was bortezomib refractory) and *in vitro* demonstrated marked synergy with the combination of BC2059 and bortezomib with an SQ = 8.2.

BC2059 blocks β-catenin/TCF transcriptional activity, promotes the destruction of β-catenin protein, and shows specificity for β-catenin

To evaluate the capacity of BC2059 to block β-catenin/TCF transcriptional activity in multiple myeloma, we transfected KMS11 with Super TOP-FLASH (wild-type TCF/LEF) and Super FOP-FLASH (mutant TCF/LEF) Wnt reporter plasmids. Upon treatment of KMS11 cells with rhWnt3a, contemporaneous exposure to BC2059 (IC_{50}: 215 nmol/L) resulted in a statistically

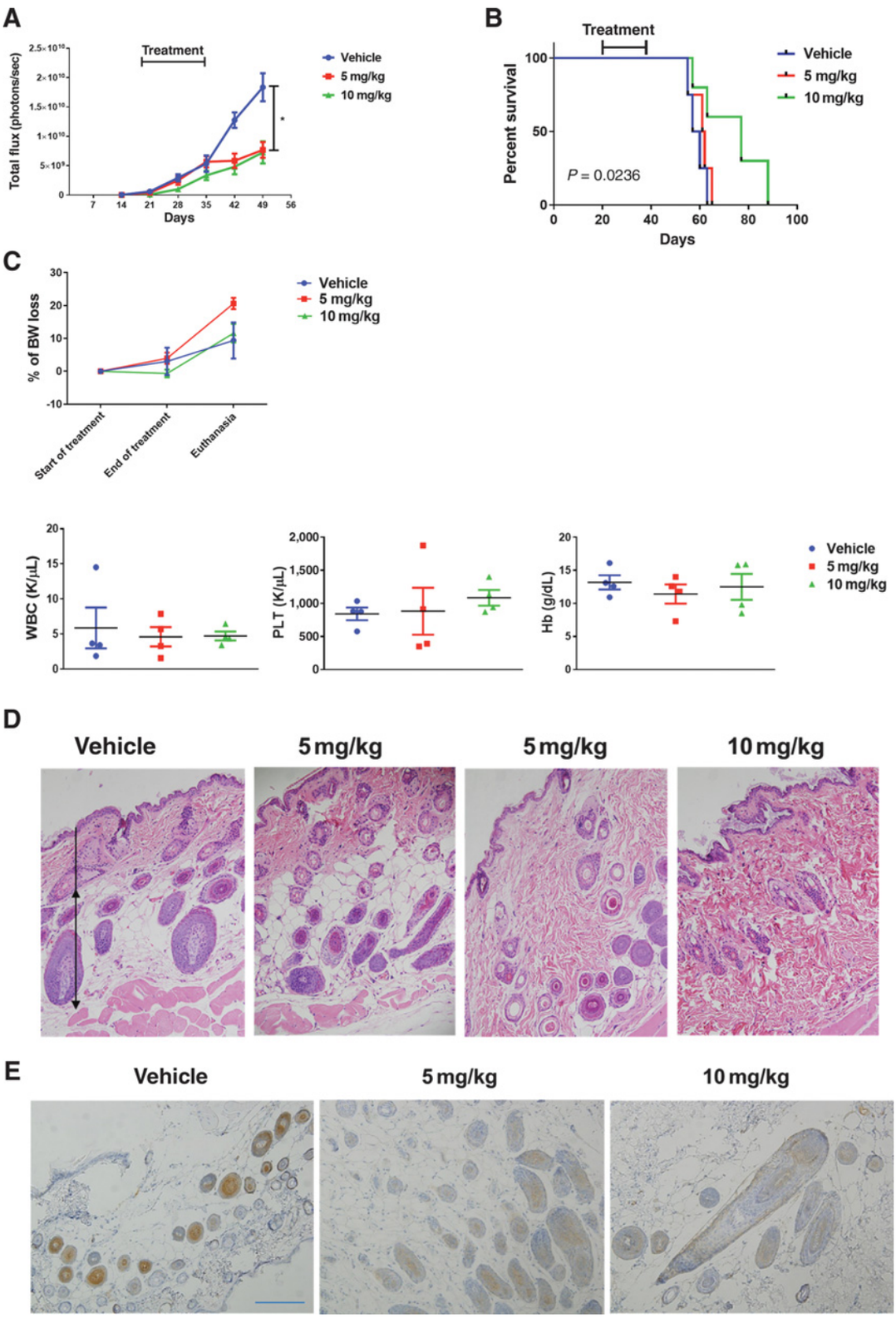

significant dose-dependent reduction in β-catenin–specific transcriptional activity (Fig. 4A). A desired characteristic of potential Wnt inhibitors will be their ability to block transcriptional activity without interfering with the destruction of β-catenin in the cytoplasm by the destruction complex. Therefore, we tested the effect of BC2059 on β-catenin protein levels utilizing the BC2059-sensitive cell line KMS18. KMS18 cells (2×10^5/mL) were treated for 16 hours with two doses of BC2059 (IC_{50} and $1.5 \times IC_{50}$, IC_{50}: 73 nmol/L), and reduction of the cell number was monitored (Fig. 4B). Similarly, KMS18 cells were treated with the same doses, and the level of whole-cell, cytoplasmic, and nuclear β-catenin levels was then quantified following immunoblotting and densitometry (Fig. 4C and D). Treatment with BC2059 at $1.5 \times IC_{50}$ resulted in a decrease in whole-cell β-catenin to almost 50% of baseline (0.54 ± 0.16) and a >50% reduction in nuclear β-catenin (total β-catenin; reduced to 0.48 ± 0.03 of baseline). This was associated with a marked reduction in transcription of the downstream β-catenin transcriptional target *AXIN2* (0.22 ± 0.16 of baseline; Fig. 4E). A similar reduction of whole-cell β-catenin protein was monitored in two additional HMCLs tested (NCI H929, U266, with IC_{50}: 173 nmol/L and 186 nmol/L, respectively) upon treatment with escalating doses of BC2059 (Fig. 5A), causing significant reduction in transcription of β-catenin target genes *AXIN2* (Fig. 5B, top) and *BIRC5* (survivin) at $1.5 \times IC_{50}$ (Fig. 5B, bottom).

Knockdown of β-catenin in the sensitive cell line KMS18 for 72 hours was able to diminish the cytotoxic effect of the drug (Fig. 5C, left), whereas immunoblotting of the UT cell lysates at the same time point confirmed decreased expression of the protein (Fig. 5C, right).

BC2059 demonstrates anti–multiple myeloma activity *in vivo* and has minimal toxicities

We then evaluated the *in vivo* effect of BC2059 utilizing a xenograft murine model of systemic human myelomatosis. NSG mice were transplanted (intravenously) with U266 HMCL stably expressing GFP and luciferase2. After 3 weeks, when disease was established in all cases, the mice were treated with vehicle alone, 5 mg/kg BC2059, or 10 mg/kg BC2059 twice weekly for 3 consecutive weeks (days 21–39, 6 doses in total). Tumor burden was monitored on a weekly basis with *in vivo* bioluminescence imaging after intraperitoneal injection of luciferin, and the median flux (photons/sec) of dorsal and ventral views for each mouse was sequentially documented. Upon the development of signs of disease, the mice were euthanized and tissues (skin and colon) collected for histopathologic studies. The mice treated with 5 mg/kg showed a significant delay of tumor growth compared with vehicle only after the termination of treatment ($P = 0.0085$ and $P = 0.0078$ in day 46 and day 53, respectively), whereas mice treated with 10 mg/kg of BC2059 demonstrated a significantly slower rate of tumor growth since the beginning of the treatment (with the exception of day 39; $P = 0.014$, $P = 0.016$, $P = 0.0038$, and $P = 0.0075$ in days 25, 32, 46, and 53, respectively; Fig. 6A). Moreover, mice treated with the higher dose of BC2059 (10 mg/kg) even with a total of only 6 doses of BC2059 demonstrated superior survival ($P = 0.024$) when compared with the vehicle cohort (Fig. 6B). Importantly, treatment with BC2059 did not result in either weight loss or peripheral blood cytopenias (Fig. 6C) when compared with vehicle-treated mice.

Finally, in view of the importance of the Wnt/β-catenin pathway on the homeostasis of adult skin and intestine, we performed IHC studies of the dorsal skin and colon harvested at the time of euthanasia. Interestingly, although we did not notice any macroscopic skin changes, the biopsies from treated mice showed dose-dependent stalling of the hair cycle process after involution with variable recycling of hair occurring. At 5 mg/kg, the process was patchy, whereas at 10 mg/kg, the process was more diffuse with concurrent fibrosis and loss of the dermal adipocyte tissue (Fig. 6D), consistent with an on-target cutaneous effect of BC2059 due to downregulation of β-catenin expression in hair follicle cells (Fig. 6E). In contrast, no significant histologic changes were seen in the gastrointestinal tract of the drug-treated mice (Supplementary Fig. S3).

Discussion

The etiology of a range of diverse malignancies, including hematologic neoplasms, may be attributable, at least in part, to Wnt canonical pathway dysregulation (4, 22–24). Furthermore, although β-catenin expression is normally lost in healthy differentiated B-lineage plasma cells, its expression, and transcriptional activity in conjunction with TCF is maintained through a yet unknown mechanism in some multiple myeloma cells (8, 10). The presence of high levels of nuclear β-catenin (active form) in all of the HMCLs that we tested is consistent with the latter and implies that upregulation of the Wnt pathway may be a common, albeit probably late (11), event in the progression of multiple myeloma irrespective of the underlying genetic make-up of the disease. We demonstrated, in accordance with previous published data (8, 12), that the Wnt canonical pathway in multiple myeloma can be further stimulated with the addition of Wnt3a (Fig. 2E), promoting the proliferation of the multiple myeloma cells and is consistent with an intact Wnt pathway. Furthermore, our finding that enhanced activation of the Wnt pathway confers further growth and survival advantage to

Figure 6.
In vivo efficacy of BC2059. **A,** Tumor growth was monitored weekly by *in vivo* bioluminescence imaging. The median flux (photons/second) of dorsal and ventral views for each cohort is documented. Multiple *t* tests (between vehicle and 5 mg/kg or vehicle and 10 mg/kg for each time point) were used for statistical analysis without assuming SD, and statistical significance was determined using the Holm–Sidak method, with $\alpha = 5.000\%$. At the last bioluminescence measurement (day 53), tumor burden for both 5 and 10 mg/kg cohorts was significantly lower than the vehicle ($P = 0.0078$ and $P = 0.0075$, respectively). **B,** NSG human multiple myeloma–bearing mice were treated with 5 or 10 mg/kg of BC2059 or vehicle alone. Kaplan–Meier survival curves of the three cohorts are shown (log-rank test for trend performed, $P = 0.023$). **C,** BC2059 treatment did not affect the body weight (BW) loss and the hematopoiesis of the multiple myeloma–bearing mice. Two-way ANOVA was used for statistical analysis, and no significant difference in bodyweight loss was found between the groups throughout the progress of the disease. At the time of euthanasia, blood was collected and complete cell count was performed. One-way ANOVA was used for statistical analysis, and no significant difference was found between the cohorts. **D,** H&E staining of mice dorsal skin revealed the effects of BC2059 in skin homeostasis, with a dose-dependent decrease of the hypodermis (black arrow), dysregulation of the normal hair growth cycle, and increase of the dermis (black line). **E,** IHC staining of mice dorsal skin with β-catenin antibody.

multiple myeloma is in accordance with previously published data (8, 10) and provides a strong basis to evaluate blockade of the Wnt pathway as a potential therapeutic modality for the treatment of multiple myeloma.

We demonstrated that BC2059 exposure reduced nuclear β-catenin protein levels in a dose- and time-dependent manner and specifically impaired β-catenin/TCF transcriptional activity without any evidence of interference, based on the reduction in the overall cellular level of β-catenin, of β-catenin binding to its destruction complex. According to previously published data (16), the drug interferes with the interaction of β-catenin with TBL1–TBLR1, which are uniformly expressed in HMCL (Supplementary Fig. S4) and which have a dual role of facilitating the transcriptional activity of the former (18), as well as protecting it from Siah-1–mediated degradation both in the nucleus and cytoplasm (20). Thus, BC2059 not only decreases the transcription of β-catenin target genes, but also decreases the levels of β-catenin in both cellular compartments. In addition, BC2059 initiation of apoptosis (Fig. 1E and F) and activation of caspases in HMCL further facilitates the destruction of β-catenin (25). The potent antiproliferative effect of BC2059 on a range of diverse HMCL after a single dose was a clear demonstration of the impact of this capacity in inhibiting the Wnt pathway. However, as the Wnt canonical pathway is essential for the homeostasis of a variety of tissues, such as skin and hair follicles, the intestinal mucosa, and the hematopoietic system, via maintenance of their stem cell pool, strategies to utilize the minimally effective doses of Wnt/β-catenin inhibitors in the clinic are required. The proliferation and viability of the HMCL were significantly inhibited in a time- and dose-dependent manner, with IC_{50} ranging from 40 to 250 nmol/L, corresponding to likely clinically achievable concentrations. Knowing that tumor–microenvironment interaction can confer drug resistance to multiple myeloma and following the recommendation that *in vitro* screening of anti–multiple myeloma agents should incorporate assays including the presence of nonmalignant accessory cells (2), we next evaluated the effect of BC2059 on HMCL when cultured with non–multiple myeloma stromal cells. For all the HMCLs tested, BC2059 at IC_{80} was able to mitigate the protective effect provided by the stroma. This activity was then recapitulated with the demonstration that approximately 50% of primary multiple myeloma tumors in an autologous bone marrow coculture displayed >50% cell death with <1 μmol/L of BC2059 when used as a single agent. However, BC2059 showed minimal effect on PBMCs, which are negative for active nuclear β-catenin (Fig. 1G), and on HS5 stromal cells (Fig. 2B and C), proving specificity of the drug. Furthermore, partial decrease of the protein by siRNA knockdown was able to decrease the cytotoxic effect of the drug (Fig. 5C). Because of the complex and context-specific mechanisms that govern the Wnt/β-catenin pathway and the possible compensatory routes for persistent β-catenin/TCF4–regulated transcription, primarily lowering β-catenin levels is not, as might be expected, enough to fully abrogate the effect of the drug. This is further supported by the absence of a direct correlation between total and/or nuclear level of β-catenin and HMCL IC_{50} to BC2059. Finally, based on previous data demonstrating the existence of possible paracrine stimulation of multiple myeloma cells within the bone marrow microenvironment mediated by secreted Wnt ligands, we tested the effect of BC2059 in the presence of multiple myeloma patient-derived stromal cell CM and rhWnt3a. In both instances, BC2059 was able to abrogate, in a dose-dependent manner, the proliferative stimulus provided to the multiple myeloma cells. In contrast, exposure to rhWt5a provided no proliferative benefit to the HMCL, thus demonstrating the pathway specificity (canonical vs. noncanonical) of Wnt dysregulation in promoting multiple myeloma growth and survival. Collectively, considering the complexity and tissue specificity of the Wnt canonical pathway, these results demonstrate specificity for BC2059, albeit minor off-target effects cannot be totally excluded.

β-catenin upregulation has been correlated with bortezomib resistance providing a clear rationale for the combination of BC2059 with bortezomib to enhance the anti–multiple myeloma effect with the least possible toxicity (26). Accordingly, the addition of bortezomib to BC2059 proved to be synergistic against the HMCLs and the primary multiple myeloma cells tested; moreover, in one case, absolute *in vivo* resistance to bortezomib confirmed in the clinical setting was partly overcome *ex vivo* by the addition of BC2059. Taken together, these results suggest that bortezomib resistance, that may in part be attributable to β-catenin upregulation, may be overcome by the addition of BC2059.

Finally, the use of BC2059 *in vivo* prolonged the survival of multiple myeloma–bearing mice, with only a brief therapeutic exposure (six doses totally). Furthermore, the effect of BC2059 impacted the growth kinetics of the disease in an ongoing fashion even after the termination of therapy, with slower tumor growth especially for the 10 mg/kg–treated mice through until the termination of imaging when compared with control animals (Fig. 6B). One of the biggest challenges in the development of Wnt/β-catenin pathway inhibitors is to diminish the possible on-target effects on other Wnt-dependent healthy tissues. In this context, we evaluated treated animals for clinical and histologic evidence of the on-target effects of BC2059. Multiple myeloma–bearing mice objectively tolerated the treatment well, with no major hair loss or differences in body weight between the cohorts, the latter consistent with functional integrity of the gastrointestinal track. Furthermore, colon biopsies did not reveal any major changes attributable to Wnt/β-catenin inhibition. In contrast, skin biopsies demonstrated dose-dependent dysregulation of normal hair cycling with a concomitant reduction in adipose tissue (hypodermis) and increased thickness of the dermis. It has been already shown (27) that inhibition of the epidermal Wnt/β-catenin signaling reduces adipocyte differentiation in the adult mouse dermis. This negatively affects the synchronized adipocyte differentiation and hair growth cycle, which follow an oscillating pattern throughout adult life. Our findings recapitulated this. Importantly, however, BC2059 treatment did not have any deleterious effect on hematopoiesis as evidenced by the absence of any emergent cytopenias in the treated groups. Although pathologic bone fractures were not noticed on the treated mice, knowing the importance of the pathway for the bone homeostasis (28–30), further investigation is currently under way.

Inhibition of dysregulated Wnt/β-catenin signaling at different levels has been demonstrated to inhibit the growth and survival of multiple myeloma cells (8, 10, 21, 31–35). However, available evidence would suggest that targeting the transcriptional activity of β-catenin with BC2059 may be able to overcome the context-specific variability and possible compensatory mechanisms that

mitigate the efficacy of alternative approaches. Collectively, our results demonstrate that BC2059 has significant anti–multiple myeloma effects against genetically heterogeneous HMCLs and primary multiple myeloma tumors in a range of *in vitro* and *in vivo* models, synergizes with bortezomib, and displays clear evidence of on-target effects *in vivo*, warranting further evaluation of BC2059 as a potential novel anti–multiple myeloma therapeutic.

Disclosure of Potential Conflicts of Interest

S. Horrigan is the chief scientific officer at and has ownership interest (including patents) in BetaCat Pharmaceuticals. No potential conflicts of interest were disclosed by the other authors.

Authors' Contributions

Conception and design: I. Savvidou, T. Khong, A. Spencer
Development of methodology: I. Savvidou, T. Khong, A. Cuddihy, S. Horrigan, A. Spencer
Acquisition of data (provided animals, acquired and managed patients, provided facilities, etc.): I. Savvidou, T. Khong, A. Cuddihy, C. McLean, A. Spencer
Analysis and interpretation of data (e.g., statistical analysis, biostatistics, computational analysis): I. Savvidou, T. Khong, A. Cuddihy, C. McLean, A. Spencer
Writing, review, and/or revision of the manuscript: I. Savvidou, T. Khong, S. Horrigan, A. Spencer
Administrative, technical, or material support (i.e., reporting or organizing data, constructing databases): I. Savvidou, T. Khong

Acknowledgments

We thank Monash Histology Platform and AMREP Flow Cytometry Core Facility.

Grant Support

This work was supported by the Monash University (Melbourne, Victoria, Australia) and Australian Centre for Blood Diseases, Monash University/Alfred Hospital (Melbourne, Victoria, Australia).

The costs of publication of this article were defrayed in part by the payment of page charges. This article must therefore be hereby marked *advertisement* in accordance with 18 U.S.C. Section 1734 solely to indicate this fact.

Received September 30, 2016; revised January 24, 2017; accepted May 3, 2017; published OnlineFirst May 12, 2017.

References

1. Palumbo A, Anderson K. Multiple myeloma. N Engl J Med 2011;364:1046–60.
2. Mitsiades C, Davies F, Laubach J, Joshua D, San Miguel J, Anderson K, et al. Future directions of next generation novel therapies, combination approaches, and the development of personalized medicine in myeloma. J Clin Oncol 2011;29:1916–23.
3. Luis TC, Ichii M, Brugman MH, Kincade P, Staal FJ. Wnt signalling strength regulates normal hematopoiesis and its deregulation is involved in leukemia development. Leukemia 2012;26:414–21.
4. Anastas JN, Moon RT. WNT signalling pathways as therapeutic targets in cancer. Nat Rev Cancer 2013;13:11–26.
5. Mikesch JH, Steffen B, Berdel WE, Serve H, Müller-Tidow C. The emerging role of Wnt signaling in the pathogenesis of acute myeloid leukemia. Leukemia 2007;21:1638–47.
6. Coluccia AML, Vacca A, Dunach M, Mologni L, Redaelli S, Bustos VH, et al. Bcr-Abl stabilizes β-catenin in chronic myeloid leukemia through its tyrosine phosphorylation. EMBO J 2007;26:1456–66.
7. Lu D, Zhao Y, Tawatao R, Cottam HB, Sen M, Leoni LM, et al. Activation of the Wnt signaling pathway in chronic lymphocytic leukemia. PNAS 2004;101:3118–23.
8. Derksen PW, Tjin E, Meijer HP, Klok MD, MacGillavry HD, van Oers MH, et al. Illegitimate WNT signaling promotes proliferation of multiple myeloma cells. Proc Natl Acad Sci U S A 2004;101:6122–7.
9. MacDonald B, Tamai K, He X. Wnt/β-catenin signaling: components, mechanisms, and diseases. Dev Cell 2009;17:9–26.
10. Sukhdeo K, Mani M, Zhang Y, Dutta J, Yasui H, Rooney MD, et al. Targeting the β-catenin/TCF transcriptional complex in the treatment of multiple myeloma. Proc Natl Acad Sci U S A 2007;104:7516–21.
11. Kocemba K, Groen R, van Andel H, Kersten MJ, Mahtouk K, Spaargaren M, et al. Transcriptional silencing of the Wnt-antagonist DKK1 by promoter methylation is associated with enhanced Wnt signaling in advanced multiple myeloma. PLoS One 2012;7:e30359.
12. Qiang YW, Endo Y, Rubin JS, Rudikoff S. Wnt signalling in B-cell neoplasia. Oncogene 2003;22:1536–45.
13. Chim CS, Pang R, Fung TK, Choi CL, Liang R. Epigenetic dysregulation of Wnt signalling pathway in multiple myeloma. Leukemia 2007;21:2527–36.
14. Huang HJ, Zhou LL, Fu WJ, Zhang CY, Jiang H, Du J, Hou J. β-catenin SUMOylataion in the dysregulated proliferation of myeloma cells. Am J Cancer Res 2015;5:309–20.
15. Driscoll JJ, Pelluru D, Lefkimmiatis K, Fulciniti M, Prabhala RH, Greipp PR, et al. The sumoylation pathway is dysregulated in multiple myeloma and is associated with adverse patient outcome. Blood 2010;115:2827–34.
16. Fiskus W, Sharma S, Saha S, Shah B, Devaraj SGT, Sun B, et al. Preclinical efficacy of combined therapy with novel β-catenin antagonist BC2059 and histone deacetylase inhibitor against AML cells. Leukemia 2015;29:1267–78.
17. Yoon H, Chan D, Huang ZQ, Li J, Fondell JD, Qin J, et al. Purification and functional characterization of the human N-CoR complex: the roles of HDAC3, TBL 1 and TBLR1. EMBO J 2003;22:1336–446.
18. Li J, Wng CY. TBL1-TBLR1 and beta–catenin recruit each other to Wnt target-gene promoter for transcription activation and oncogenesis. Nat Cell Biol 2008;10:160–9.
19. Choi HK, Choi KC, Yoo JY, Song M, Ko SJ, Kim CH, et al. Reversible SUMOylation of TBL1-TBLR1 regulates beta-catenin-mediated Wnt signalling. Mol Cell 2011;43:203–16.
20. Dimitrova YN, Li J, Lee YT, Rios-Esteves J, Friedman DB, Choi HJ, et al. Direct ubiquitination of beta-catenin by Siah-1 and regulation by the exchange factor TBL1. J Biol Chem 2010;285:13507–16.
21. Yao H, Ashihara E, Strovel JW, Nakagawa Y, Kuroda J, Nagao R, et al. AV-65, a novel Wnt/β-catenin signal inhibitor, successfully suppress progression of multiple myeloma in a mouse model. Blood Cancer J 2011;e43:1–9.
22. Clevers H, Barker N. Mining the Wnt pathway for cancer therapeutics. Nat Rev 2006;5:997–1014.
23. Reya T, Clevers H. Wnt signalling in stem cells and cancer. Nature 2005;434:843–9.
24. Ysebaert Y, Chicanne G, Demur C, De Toni F, Prade-Houdellier N, Ruidavets JB, et al. Expression of beta-catenin by acute myeloid leukaemia cells predicts enhanced clonogenic capacities and poor prognosis. Leukemia 2006;20:1211–6.
25. Steinhusen U, Badock V, Bauer A, Behrens J, Wittman-Liebold B, Dörken B, et al. Apoptosis-induced cleavage of beta-catenin by caspase-3 results in proteolytic fragments with reduced transactivation potential. J Biol Chem 2000;275:16345–53.
26. Zhou L, Hou J, Fu W, Wang D, Yuan Z, Jiang H. Arsenic trioxide and 2methoxyestradiol reduce β-catenin accumulation after proteasome inhibition and enhance the sensitivity of myeloma cells to Bortezomib. Leuk Res 2008;32:1674–83.
27. Donati G, Proserpio V, Lichtenberger BM, Natsuga K, Sinclair R, Fujiwara H, et al. Epidermal Wnt/β-catenin signalling regulates adipocyte differentiation via secretion of adipogenic factors. Proc Natl Acad Sci U S A 2014;111:E1501–9.
28. Noll JE, Williams SA, Purton LE, Zannettino AC. Tug of war in the haematopoietic stem cell niche: do myeloma plasma cells compete for the HSC niche? Blood Cancer J 2012;2:e91.
29. Edwards CM, Edwards JR, Lwin ST, Esparza J, Oyajobi BO, McCluskey B, et al. Increasing Wnt signaling in the bone marrow microenvironment

inhibits the development of myeloma bone disease and reduces tumor burden in bone in vivo. Blood 2008;111:2833–42.
30. Qiang YW, Shaughnessy JD, Yaccoby S. Wnt3a signalling within bone inhibits multiple myeloma bone disease and tumor growth. Blood 2008;112:374–82.
31. Schmidt M, Sievers E, Endo T, Lu D, Carson D, Schmidt-Wolf IG. Targeting Wnt pathway in lymphoma and myeloma cells. Br J Haematol 2009; 144:796–8.
32. Kim Y, Reifenberger G, Lu D, Endo T, Carson DA, Gast SM, et al. Influencing the Wnt signaling pathway in multiple myeloma. Anticancer Res 2011;31:725–30.
33. Kim Y, Schmidt M, Endo T, Lu D, Carson D, Schmidt-Wolf IG. Targeting the Wnt/beta-catenin pathway with the antifungal agent ciclopiroxolamine in a murine myeloma model. In Vivo 2011;25:887–93.
34. Park S, Yun E, Hwang IH, Yoon S, Kim DE, Kim JS, et al. Ilimaquinone and Ethylsmenoquinone, marine sponge metabolites, supress the proliferation of multiple myeloma cells by down-regulating the level of β-catenin. Mar Drugs 2014;12:3231–44.
35. Grigson ER, Ozerova M, Pisklakova A, Liu H, Sullivan DM, Nefedova Y. Canonical Wnt pathway inhibitor ICG-001 induces cytotoxicity of multiple myeloma cells in Wnt independent manner. PLoS One 2015;10: e0117693.